Desalination and Water Treatment
www.deswater.com

doi:10.5004/dwt.2018.22478

116 (2018) 19–28
June

Enhancement in permselectivity and antibacterial performances of polyamide RO membranes via surface modification of AgCl nanoparticles

Hao Li, Dongbing Cheng*, Lingyao Dong, Feng Qian

Changjiang River Scientific Research Institute, Huangpu Street, Wuhan 430072, PR China, Tel. +86 18064111112, Fax +86-27-82920797, email: haol@whu.edu.cn (H. Li), Tel. +86 13100625130, email: xiao2005zhu@163.com (D. Cheng), Tel. +86 15717160712, email: 34425685@qq.com (L. Dong), Tel. +86 15827408850, email: 402483315@qq.com (F. Qian)

Received 22 November 2017; Accepted 5 May 2018

ABSTRACT

Membrane fouling, especially bio-fouling, limits the further development of thin film composite (TFC) aromatic polyamide reverse osmosis (RO) membranes. In the current study, a simple method (the alternative soaking surface mineralization technique) was used to deposit AgCl particles onto surfaces of commercial RO membranes to enhance its antibacterial performance and permselectivity simultaneously. Scanning electron microscopy (SEM) and X-ray photoelectron spectroscopy (XPS) confirmed the deposition of AgCl particles on the surface of the modified membranes. Characterization of membrane surface showed the modification enhanced the hydrophilic of membrane surfaces, made the membrane surfaces more negatively charged and did not influence the membrane surface roughness. Under RO operation, the modification improved the membrane flux and salt rejection. Membrane fouling test showed the modified membranes had slower water flux decline rate and higher water flux recovery rate. Membrane antibacterial test showed the death rates of Escherichia coli after contacting with modified membranes were much larger than that after contacting with the unmodified membrane.

Keywords: Reverse osmosis membrane; Surface modification; AgCl; Anti-fouling; Antibacterial

1. Introduction

The emergence of thin film composite (TFC) aromatic polyamide reverse osmosis (RO) membranes, as the milestone of the RO technology, has promoted the large-scale industrialization and application of this technology [1]. So far, this technology has been widely applied into seawater/brackish water desalination, pure/ultra pure water production, municipal/industrial wastewater treatment, and product concentrates [2,3]. However, the further development of TFC aromatic polyamide RO membranes is limited by the risk of membrane fouling [4,5]. The colloids, minerals, organic matter and microbes in the feed solution adsorb and deposit on the surfaces of the polyamide layer, and thereby interfere with the permselectivity of RO membranes, raising operational costs and shortening of membrane life [6–8]. In particular, the largest threat to the RO system is bio-fouling [9,10]. Microbes would adsorb and grow on membrane surfaces, and secrete numerous extracellular polymeric substances (EPS), which evolve into biofilms on membrane surfaces and finally induce irreversible blockage [10–13].

Numerous works have been conducted to control membrane fouling [14,15]. Especially, surface modification is one of the most effective methods [16,17]. Active groups (amido and carboxyl groups on the polyamide layer of TFC membranes) would act as intermediate to introduce modifiers onto the surface of RO membranes through physical coating, in-situ polymerization, grafting or chemical coupling [18–23]. Through the modification, the surface physicochemical properties of RO membranes such as surface hydrophilicity, surface charge, roughness are influenced by the modifiers [24], thereby enhancing anti-fouling resis-

*Corresponding author.

tance of membranes. Thus, the key of membrane surface modification is to find out the appropriate modifying material that can be introduced onto membrane surfaces.

As is well-known, Ag has strong sterilization ability against more than 600 types of bacteria and is commonly used to improve the antibacterial ability of diverse materials [25–27]. In recent years, Ag has been used into RO membrane modification. Yin et al. synthesized Ag nanoparticles (AgNPs) through a series of reactions and introduced the AgNPs onto the surfaces of self-made RO membranes with cysteamine as the intermediate [28]. Yang et al. coated Ag onto membrane surfaces through complex redoxes starting from silver nitrate, ammonia, ethanol and formaldehyde [29]. However, the above modifications modestly reduce the water flux of RO membranes. Thus, in this study, we aim to find out an appropriate method to introduce silver onto surfaces of RO membranes, without reducing the osmosis performance.

Specifically, in this study, the alternative soaking surface mineralization technique was used to deposit AgCl particles onto surfaces of commercial RO membranes. Then the effects of mineralization cycles on the amount of AgCl deposition were studied. The effects of modification on membrane surface properties (hydrophilicity, surface charge, and surface morphology) were investigated through a series of tests. The changes of membrane permselectivity after modification were explored and the stability of AgCl particles on membrane surfaces were studied. With a simulated contaminant bovine serum albumin (BSA), we investigated how modification could improve the membrane fouling resistance against organic and with *E.coli*, we tested how modification could enhance the membrane antibacterial ability.

2 Materials and methods

2.1 Chemicals and reagents

XLE-4040 (DOW; Jiangsu Hersbit Environmental Protection Technology Co. Ltd., China) was used as the original membrane. Sodium chloride (NaCl) and silver nitrate ($AgNO_3$), (both ≥99.5%, Shanghai Aladdin Reagent Co. Ltd.) were used as modifiers. BSA(≥ 96%, Shanghai Aladdin Reagent Co. Ltd.,) was used as a fouling agent in fouling experiments. *E.coli* DSM 4230 (DSMZ Braunschweig, Germany) was used as the model microbe in antibacterial experiments. Deionized water produced from two-stage reverse osmosis and electrodialysis was used as the solvent for all aqueous casting solutions. All other reagents such as hydrogen chloride, sodium hydroxide and isopropyl alcohol were analytically pure (Sinopharm Chemical Reagent Co. Ltd.) and used without further purification.

2.2. Modification of RO membranes

The alternative soaking surface mineralization technology is a simple modification technique commonly used to coat calcium salts onto surfaces of polymer materials [30,31]. In this experiment, the membranes were successively immerged into $AgNO_3$ and NaCl solutions to deposit AgCl onto surfaces of RO membranes. The mechanism is illustrated in Fig. 1.

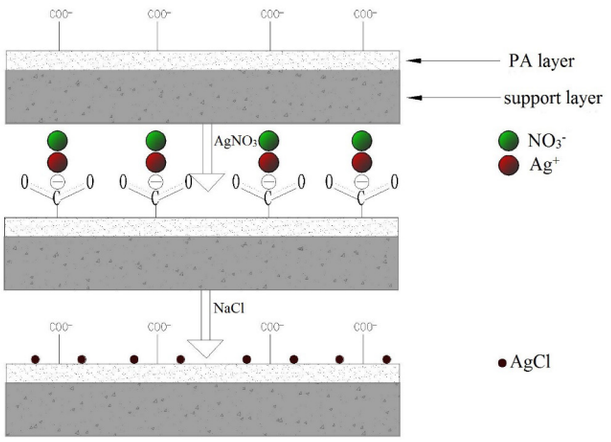

Fig. 1. Schematic of the surface modification of AgCl nanoparticles.

There were three steps. (1) XLE RO membranes were soaked for 30 min into a 30%V/V isopropanol solution, which removed the residues on membrane surfaces during the preparation process. Then the membranes were washed with deionized water and reserved in ultrapure water for more than 24 h. Water was changed every 6 h. (2) The preprocessed membranes were taken out, placed into a 0.1 mol/L silver nitrate solution for 60 s, and washed with ultrapure water for more than 60 s to remove the loosely-adsorbed Ag^+. (3) The resulting membranes were soaked in a 0.1 mol/L NaCl solution for 60 s and washed with ultrapure water for more than 60 s. Steps (2) and (3) were marked as one cycle. The unmodified membrane was named as M_0 and the membrane after n cycles of modification was marked as M_n. The deposition degree of AgCl on membrane surfaces was evaluated by mineralization degree (MD). Specifically, every test membrane was repeatedly washed with ultrapure water, vacuum-dried at 50°C and continuously weighed until the weight was unchanged. MD (g/m^2) was computed as follows:

$$MD = \frac{(W_1 - W_0)}{A} \quad (1)$$

where W_0—weight of an RO membrane before modification (g); W_1—weight of an RO membrane after modification (g); A—area of an RO membrane (m^2).

2.3. Surface characterization of RO membranes

The unmodified and modified membranes were vacuum-dried at 50°C for 2 h, followed by surface characterization. Contact angle was measured by a JC2000D2 contact angle instrument (Shanghai Zhongchen Digital Technology Co., Ltd.). During each measurement, 2 µl of ultrapure water was dripped onto membrane surfaces. The spread of liquid drips on membrane surfaces was photographed every 5s. The contact angle between the drip tip and the bottom was computed on software. Each measurement lasted 50 s. Each type of membranes was measured at least 5 times. Surface morphology was detected on a field-emis-

sion scanning electron microscope (FESEM, Sigma, Zeiss). Before testing, the processed samples were sprayed with gold to enhance electroconductivity. The changes of *element* composition on membrane surfaces were detected by an ESCALAB 250Xi X-ray photoelectron energy spectrum meter (XPS, Thermo Fisher Scientific, America): monochromeAlKα crystals as the emission source; step length of full-spectrum analysis = 1 eV/step; single element analysis = 0.1 eV/step. The Ag amount on membrane surfaces was detected by energy dispersive spectrometry (EDS), an attachment of SEM. Membrane surface roughness was measured by an SPM-9500J3 AFM instrument (Shimadzu, Japan) in the noncontact mode and quantified by average roughness (Ra) and root-mean-square (Rms). Surface charge was detected by Zeta potential measurement on a surpass Zeta potential instrument (Anton Paar GmbH, Austria): 0.01 mmol/L KCl solution as the electrolyte solution; 0.1 mol/L HCl and KOH solutions for pH adjustment within the range pH 3–10; operation pressure = 0.1–0.5 Mpa; 25±0.2°C.

2.4. Permselectivity evaluation of RO membranes

The permselectivity of membranes was evaluated through a laboratory scale cross-flow test unit. The details of this cross-flow unit have already been published in one of our previous works [32]. The water flux and salt rejection were tested in a 1000 ppm NaCl solution at 1 MPa and 25°C. The water flux and salt rejection were calculated as follows:

$$\text{Water flux} = \frac{\text{permeate volume}(\text{L})}{\text{membrane area}(\text{m}^2) \times \text{time}(\text{hours})} \quad (2)$$

$$\text{Salt rejection}(\%) = \left(1 - \frac{\text{concentration of permeation}}{\text{concentration of feed solution}}\right) \times 100 \quad (3)$$

The reported values are averages obtained from at least three samples for each type of membranes.

2.5. Antifouling property evaluation of RO membranes

With the commonly-used simulated contaminant BSA [18,33], we studied how modification would affect the antifouling ability of RO membranes. The concentration of BSA was 200 ppm.

The course of membrane fouling experiments is illustrated in Fig. 2. Specifically, (1) the initial water flux of the non-contaminated membranes was tasted in a 1000 ppm NaCl solution. (2) The high-pressure pump was closed, and an appropriate amount of the membrane fouling reagent was added to the feed tank, so the contaminant solution with the target concentration was prepared. (3) After certain time of stirring, the BSA was completely dissolved. Then the high-pressure pump was opened, and the variation of membrane water flux with time was recorded. (4) After 3 h of simulated membrane fouling, the high-pressure pump was closed. The membrane fouling solution was exchanged to deionized water. Then the high-pressure pump was opened, followed by 2 h of flushing at normal pressure. Finally, the recovery of membrane water flux was tested in a 1000 ppm NaCl solution.

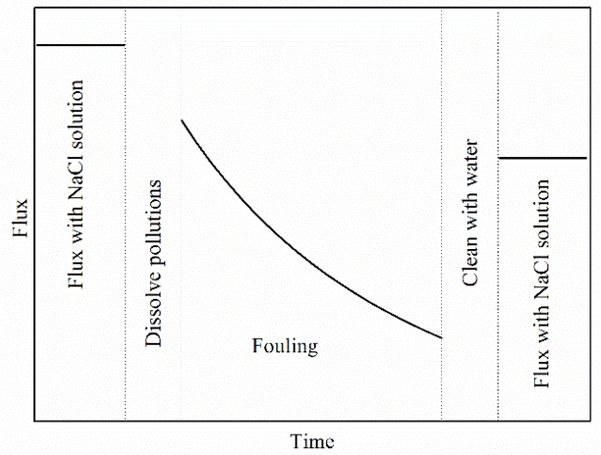

Fig. 2. Experimental protocol for the fouling/cleaning.

2.6. Antibacterial property evaluation of RO membranes

In this section, *E.coli* was used as the model microbe. *E.coli* is a Gram-negative short bacillus (0.5–1.5 μm) commonly seen in water, and is often used to measure antibacterial properties of diverse materials [34,35].

Specifically, the unmodified and modified membranes were cut into 0.5 mm^2 pieces. In the super-clean table, 10 ml of sterilized LB medium was poured into a 50 ml centrifuge tube, to which 1 ml of 2 × 10^6 cfu/ml of an *E.coli* suspension was added via a pipette. Then 0.2 g of membrane pieces was added into the bacterial solution, which was then put into a thermostat water bath oscillation box for timed cultivation (36.5°C, rotation speed = 130 rpm, 30 min–4 h). Then 0.1 ml of the solution was collected at a certain interval and put into 1 ml centrifugal tubes, which were diluted 100 times via the multiple gradual increase method. Then 0.5 ml of the diluted bacterial solution was collected and added into the LB solid medium. The culture dish was slowly rotated, so the bacterial solution and medium were uniformly mixed. After the medium solidified, it was put into a thermostat water bath incubator for 24 h of cultivation, followed by observation of colony growth. Each group was tested three times and the average was obtained. The sterilization ratio (SR %) was computed as follows:

$$\text{SR}(\%) = \frac{N_0 - N_1}{N_0} \times 100 \quad (4)$$

where N_0—number of colonies per unit area in the control group; N_1—number of colonies per unit area in the test group.

3. Results and discussion

3.1. Effects of AgCl modification on membranes surface properties

3.1.1. Surface element of AgCl-modified membranes

The principle of membrane surface modification is illustrated in Fig. 1. The feasibility of the principle was validated

through the XPS results. The spectrum of unmodified membranes only showed the peaks of C1s, N1s and O1s at 284.7, 399.9 and 531.2 ev, respectively (Fig. 3). On the contrary, the spectrum of modified membranes showed five more peaks at 198.1,268.3 ev (characteristic of Cl^-) and 374.0, 367.9, 572 ev (characteristic of Ag^+). The appearance of these characteristic peaks validated the surface sedimentation of AgCl, or namely the success of modification.

Meanwhile, the MD of modified membranes were measured to study the effects of modification cycles on the amount of AgCl deposition (Fig. 4). Clearly, the MD rose with the increase of modification cycles. At the initial stage of modification, the MD was almost linearly correlated with the modification cycles, and increased from 0.148±0.0067 g/m^2 in membrane M_1 to 0.512±0.0724 g/m^2 in membrane M_4. However, with further increase of modification cycles, the MD rose at a slower rate. The probable reason was that with the increase of modification cycles, after each modification, the number of surface active sites for Ag^+ adsorption decreased, and thereby the adsorbed amount of Ag^+ on membrane surfaces and the amount of AgCl deposition on membrane surfaces all decreased.

3.1.2. Surface hydrophilicity of AgCl-modified membranes

The surface hydrophilicity largely affects the water flux and fouling resistance of RO membranes. In this study, the surface hydrophilicity of RO membranes was measured by detecting the surface contact angle in ultrapure water (Fig. 5). Clearly, with the increase of modification cycles, the contact angles of RO membranes gradually decreased by 33.7% from 66.7°±2.8° in membrane M_0 to 44.2°±2.1° in membrane M_8, indicating modification effectively promoted the surface hydrophilicity of membranes. However with the increase of modification cycles, the effect of modification on the membrane hydrophilicity was weakened after each modification. The contact angle decreased by 10.2° from membrane M_0 to membrane M_2, but only droped by 2° from membrane M_6 to membrane M_8. This was probably because with the increase of modification cycles, the amount of AgCl deposition on membrane surface gradually decreased after each modification.

3.1.3. Surface morphology of AgCl-modified membranes

Fig. 6 shows FE-SEM images of modified and unmodified membranes. Clearly, the unmodified membrane surfaces showed a peak-valley structure caused by the different interconnecting degrees. This structure was not changed after modification, but a particle-like structure, which was the crystals of AgCl deposition, appeared on membrane surfaces. This change also validated the success of AgCl depositing. Moreover, with the increase of modification cycles, the number of AgCl crystal particles deposited on membrane surfaces gradually increased, which validated the previous conclusion that the amount of deposition gradually rose with the increase of modification cycles. In

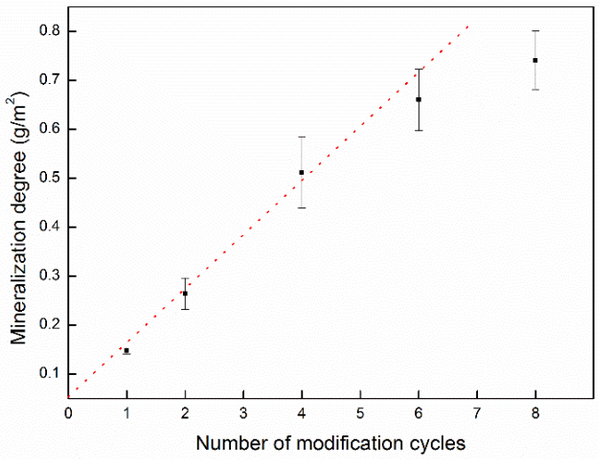

Fig. 4. Change of the mineralization degree with the number of modification cycles.

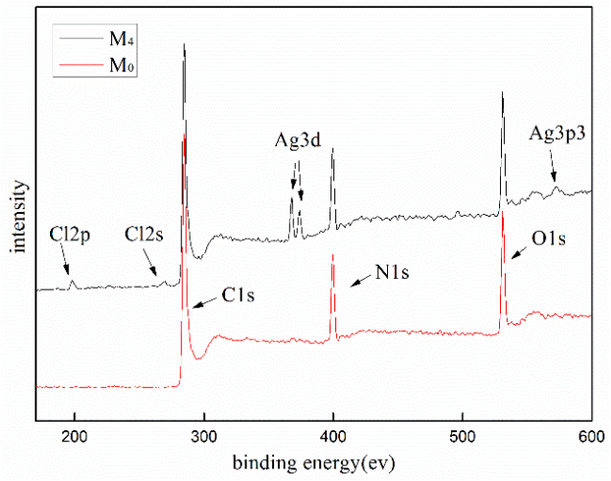

Fig. 3. XPS Spectrum of M_0 and M_4 modified membranes.

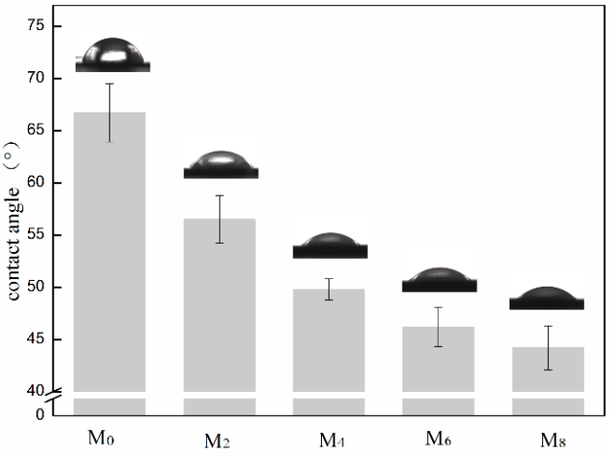

Fig. 5. Water contact angle results of unmodified and modified membranes.

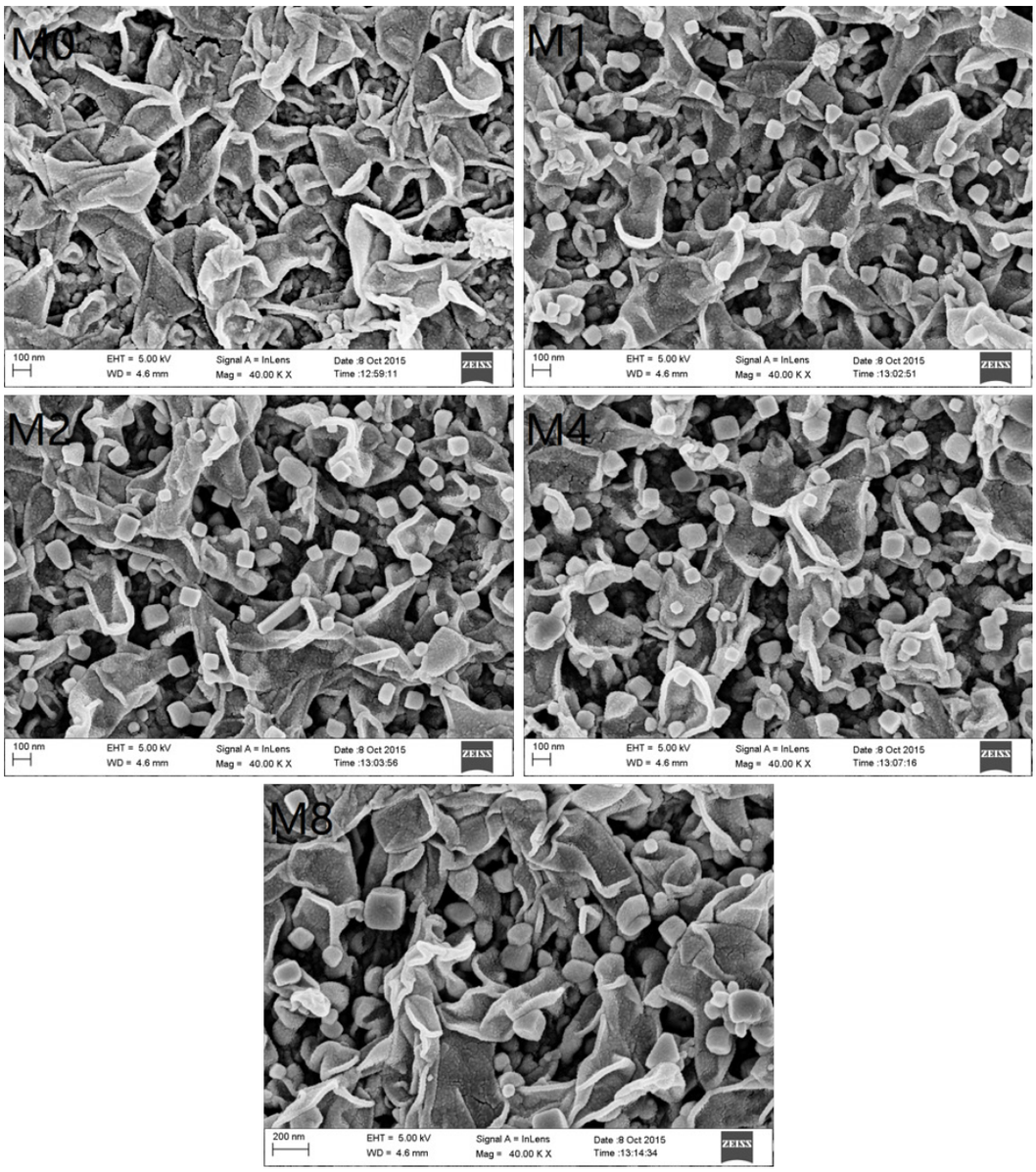

Fig. 6. SEM images of unmodified and modified membranes.

addition, with the increase of modification cycles, the sizes of AgCl crystal particles deposited on membrane surfaces were also enlarged. The crystal particle sizes on surfaces of membrane M_1 were mostly smaller than 100 nm, but the particle sizes of membrane M_8 were mostly between 100 and 200 nm, indicating the pre-deposited AgCl crystal particles could work as active sites in the following AgCl deposition. Moreover, compared with the previous Ag^+ modification, this method could introduce smaller AgCl particles onto surfaces of RO membranes. "Smaller particle size" means the surface areas are larger and can contact with more bacteria at the same deposition amount.

Moreover, we measured the AFM of unmodified membranes and modified membranes, aiming to study the effects of modification on membrane surface roughness. The surface stereo structure is illustrated in Fig. 7, and the corresponding membrane surface roughness is listed in Table 1. No significant change was noted in the surface stereo structure, Rms or Ra after modification, indicating modification did not affect the surface roughness of RO membranes.

3.1.4. Surface charge of AgCl-modified membranes

Fig. 8 illustrates the effects of modification on the surface charge of RO membranes. Due to the existence of amido and carboxyl groups, the surface Zeta potential changed with pH. Clearly, the Zeta potential of modified

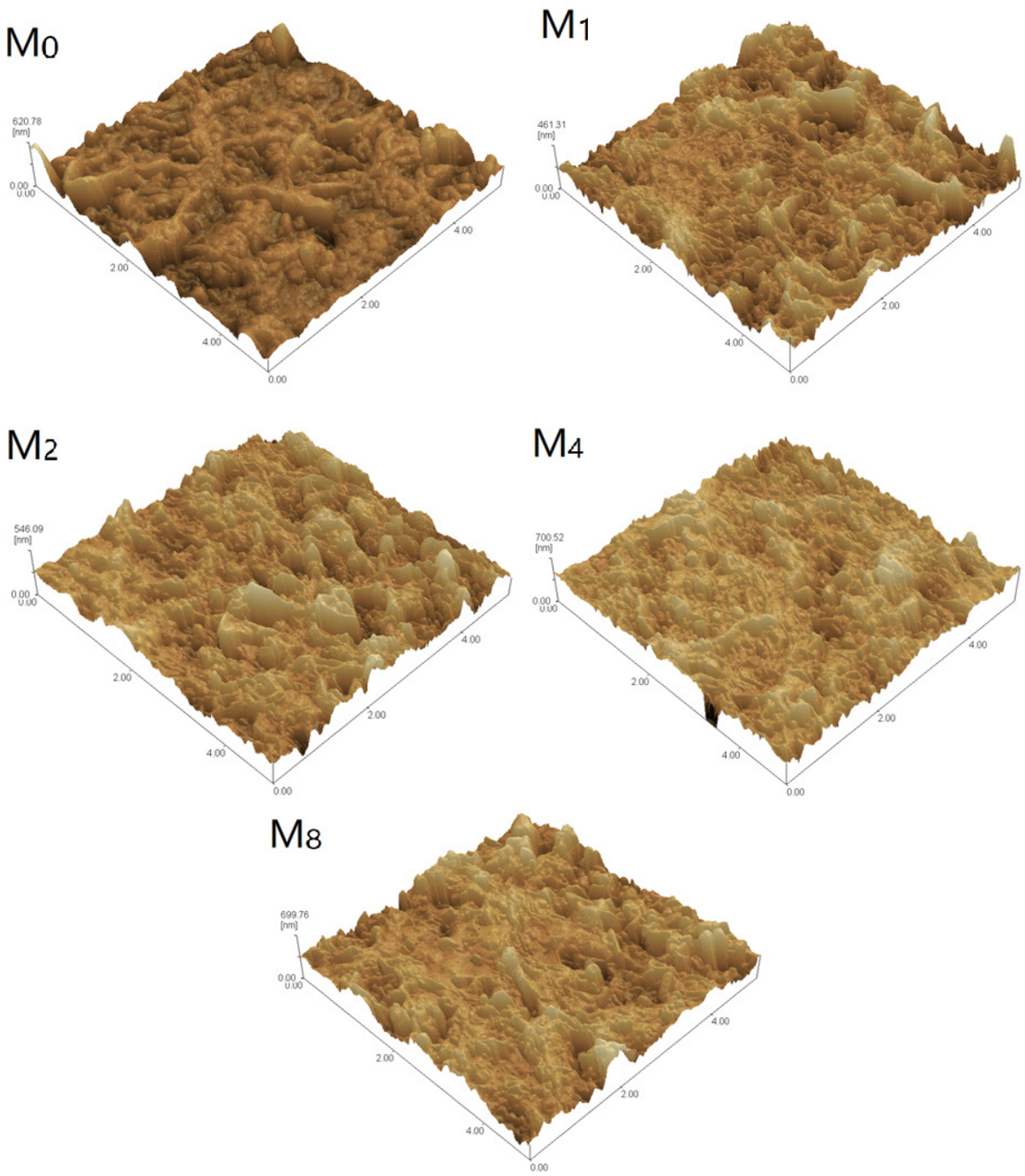

Fig. 7. AFM images of unmodified and modified membranes.

Table 1
Surface roughness of unmodified and modified membranes

Sample	Area (μm²)	Ra (nm)	Rms (nm)
M_0	25	47.13	63.01
M_1	25	47.61	60.13
M_2	25	53.07	65.82
M_4	25	50.10	62.86
M_8	25	53.37	67.42

RO membranes generally migrated to negative charge, and the negative charge was intensified with the increase of modification cycles. The isoelectric point migrated from pH=4.95 of membrane M_0 to pH=4.61 of membrane M_4 and then to pH=4.32 of membrane M_8. Such change was induced by the small amount of anion adsorbed by the deposited AgCl crystals on membrane surfaces. This result was consistent with the conclusions from Zhou [30] and Zhang [36], who studied $BaSO_4$ coating and found anions including COO^- and OH^- were adsorbed during the coating process.

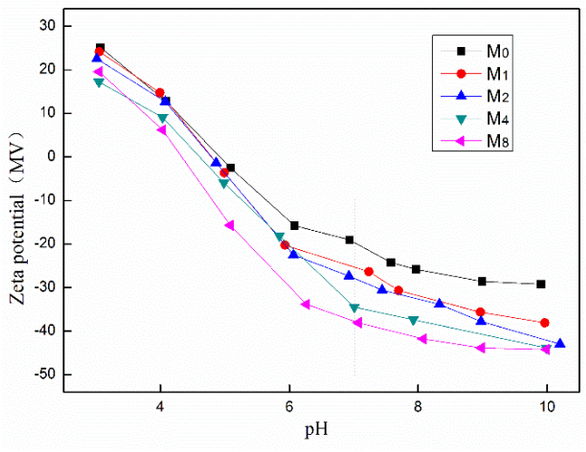

Fig. 8. Surface zeta potential results of unmodified and modified membranes.

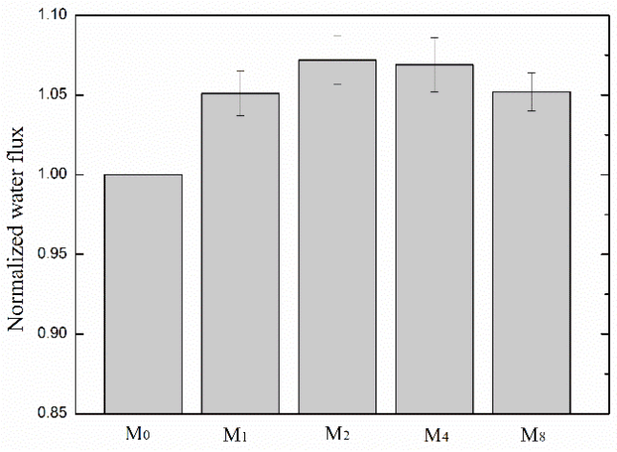

Fig. 9. Normalized water flux of unmodified and modified membranes.

3.2. Effects of AgCl modification on membrane permselectivity

Figs. 9 and 10 illustrate the effects of modification on water flux and salt rejection, two major indicators of membrane permselectivity. Different from the fact that modification usually decreases membrane flux, we found the flux of modified RO membranes slightly increased (Fig. 9). The normalized flux increased with the rise of modification cycles, as it rose from 105.1±1.4% of membrane M_1, maximized in between membrane M_2 and M_4, and then gradually declined, but was always larger than membrane M_0. According to the principle of dissolution diffusion, it was probably because (1) with the increase of modification cycles, the surface hydrophilicity of RO membranes was enhanced, which was favorable for water dissolution on membrane surfaces and induced the increase of water flux, and (2) AgCl crystals deposited on membrane surfaces, which narrowed the contact areas between water and membrane surfaces, and the amount and volume of crystals both increased with the increase of modification cycles, leading to the decrease of flux. The change of membrane flux along with the modification cycles resulted from the joint action of these two reasons.

The effects of modification on salt rejection of RO membranes are illustrated in Fig. 10. Different from the variation of flux, the salt rejection of RO membranes gradually increased with the rise of modification cycles. The above characterizations suggested there might be two causes: (1) modification intensified the membrane surface electronegativity, enhanced the charge repulsion between anion and membrane surfaces in the solutions, and thereby reduced salt flux; (2) modification enhanced water flux, reduced the salt concentration of passing through liquids under the same salt flux, thereby increased salt rejection rate. Moreover, with the increase of modification cycles, the rising rate of salt rejection was slowed down. After the first modification, the salt rejection rate increased by about 1% from 95.8±0.9% in membrane M_0 to 96.8±0.8% in membrane M_1, and then increased by only 0.4% from 97.8±1% in membrane M_4 to 98.2±0.9% in membrane M_8. This might be attributed to the slight reduction of flux along with the increase of modification cycles.

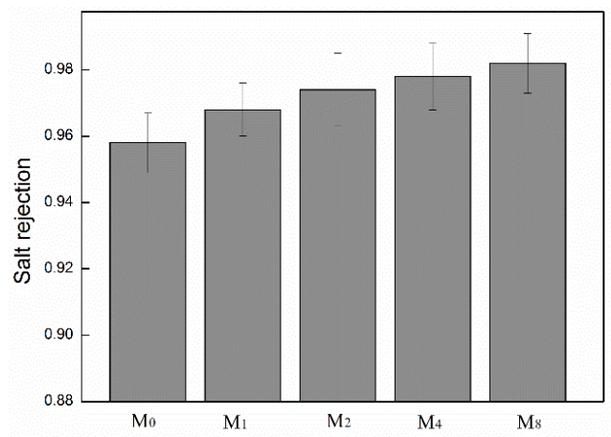

Fig. 10. Salt rejection of unmodified and modified membranes.

3.3. The stability of AgCl-modified membranes

The water flux and slat rejection of membrane M_4 were tested by using a 1000 ppm NaCl solution every half hour for 48 h (Fig. 11), to characterize the stability of AgCl deposition on membrane surfaces. Clearly, neither water flux nor salt rejection of RO membranes changed largely during the 48 h, indicating the high stability of RO membranes. In addition, another membrane M_4 was tested for 48 h by using ultrapure water for EDS characterization (Fig. 12). After 48 h of filtration, the relative concentrations of membrane surface Ag^+ only declined slightly from 0.19% to 0.18%, which was more stable than the study from Zhu et al. [37], who tested AgCl-modified RO membranes for 18 h and found the Ag coating decreased by 27%.

3.4. Effects of AgCl modification on membrane antifouling ability

With 200 ppm BSA as a simulated contaminant solution, we tested membranes M_4 and M_0 (Fig. 13). Clearly, the relative flux of M_0 decreased to 61.55% in the mem-

brane fouling tests and recovered to 80.79% after cleaning. The relative flux of M_4 decreased to 69.99% in the membrane fouling tests and recovered to 89.71% after cleaning. The previous trials suggest the membrane fouling of M_0 was a typical two-stage process [38,39]: (1) the first rapid decrease of flux was attributed to the interaction between BSA and membrane surfaces, and (2) the second rapid decrease of flux was due to the interaction between adsorption-induced BSA layers and BSA molecules. As for M_4, its flux rapidly declined at first, but no rapid decrease occurred in the remaining fouling process, indicating no valid BSA adsorption layer was formed on membrane surfaces during the whole fouling process, or namely the modification largely weakened the surface adsorption of BSA molecules. Moreover, the larger recovery of modified membranes also indicated this, so the contaminant adsorbed on membrane surfaces was more easily washed out, improving the membrane fouling resistance. Together with previous characterization and these results, the performance improvement was attributed to two reasons: (1) modification improved the surface hydrophilicity of RO membranes and reduced the hydrophobic interaction between BSA molecule aggregates and membrane surfaces, and (2) modification enhanced membrane surface electronegativity and intensified the charge repulsion between membrane surfaces and BSA molecules.

3.5. Effects of AgCl modification on membranes antibacterial ability

To study the effects of modification on antibacterial ability of membranes, we quantified the antibacterial performance of modified membranes through flat-plate counting.

The sterilization ratio of membrane M_0 and membrane M_4 during 4 h of contact are illustrated in Fig. 14. Clearly, since the original growing environment of bacteria was changed during the trials, a small amount of bacteria was killed after the contact with M_0, and the death rate after 4 h was 19.7±4.8%. As for M_4, the bacteria rapidly died after the contact with membranes, and the death rate after 30 min was 30.7±8.9%, and reached 85.2±5.2% after 4 h.

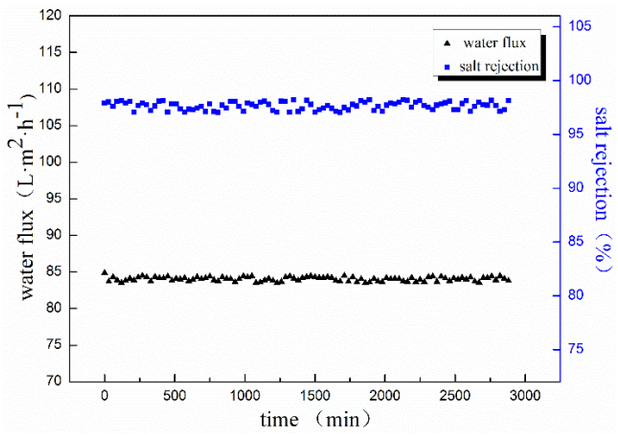

Fig. 11. Changes of salt rejection and water flux with filtration time for membrane M_4.

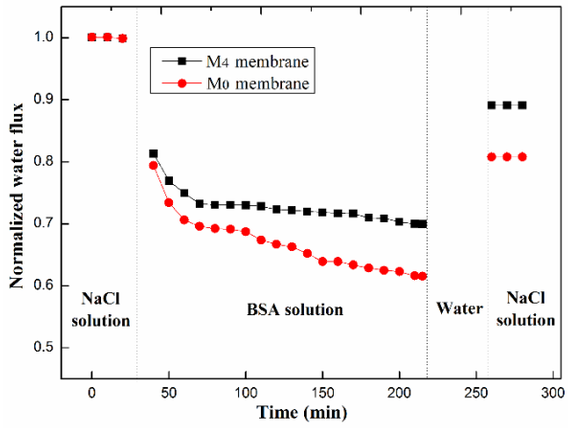

Fig. 13. Fouling and cleaning experiments of unmodified and membrane M_4.

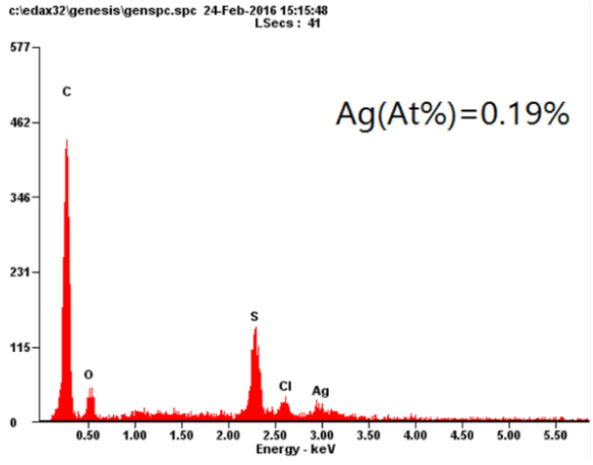

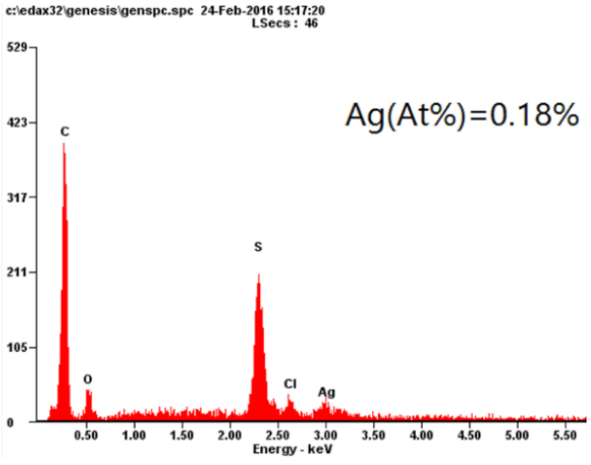

Fig. 12. EDS results of membrane M_4 before and after 48 h filtration.

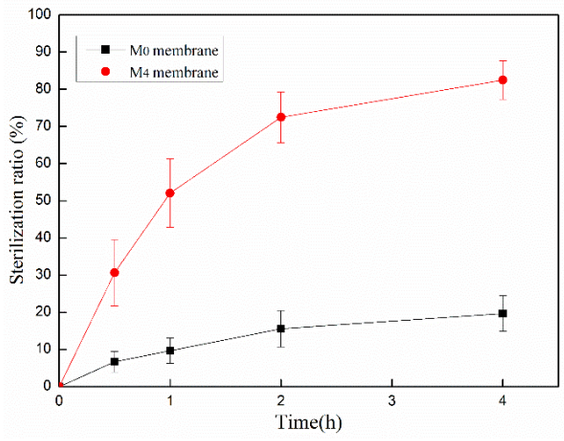

Fig. 14. Sterilization ratio of M_0 and M_4 membranes.

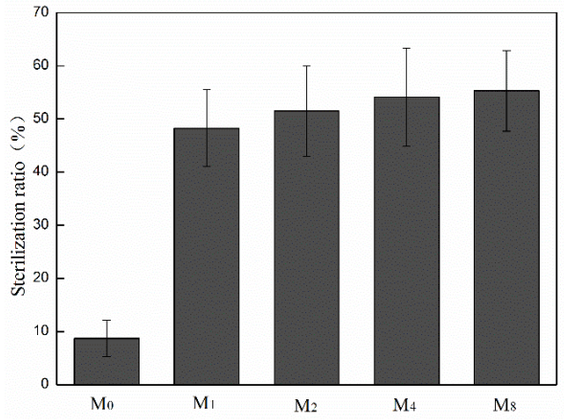

Fig. 15. Influence of modified cycles on membrane sterilization ratio.

Fig. 15 shows the sterilization ratio of unmodified and modified membranes after 1 h of contact. Clearly, a small amount of bacteria died after 1 h of contact with M_0, and the death rates of modified membranes were far larger than the unmodified membrane, due to the influence of AgCl nanoparticles on bacterial metabolism [35]. The bacterium death rates of membrane M_1 after 1 h of contact were 48.3±7.2% and gradually increased with the rise of modification cycles. However, the rising amplitude of sterilization ratio was not significant with the rise of modification cycles. After 1 h of contact with M_8, the bacterium death rate was only 55.3±7.6%. Those results indicated that modification effectively improved the antibacterial property of membranes, and only a small amount of AgCl deposition could endow the membranes with excellent antibacterial and inhibitory effect, and the increase of deposition amount did not largely improve the antibacterial effect.

4. Conclusions

The alternative soaking surface mineralization technique was used to deposit AgCl particles onto surfaces of commercial RO membranes. XPS and SEM validate the success of modification, and with the increase of modification cycles, the amount of nanoscale AgCl particles deposited on membrane surfaces gradually increases. The modified membranes displayed higher hydrophilicity and larger electronegativity than the unmodified membrane. As for permselectivity, the increase of surface hydrophilicity and the change of electronegativity jointly improve the membrane flux and salt rejection. Moreover, membrane fouling test showed the modified membranes had slower water flux decline rate and higher water flux recovery rate, which validated modification could improve the membrane fouling resistance of membranes; *E. coli* antibacterial trials showed the bacterium death rates after contact with modified membranes were far larger than with the unmodified membrane and a high antibacterial effect was achieved only by a small amount of AgCl deposition, indicating modification could improve the antimicrobial ability of membranes.

Acknowledgments

This work was supported by the National Key Research and Development Program of China (No. 2017YFC050530302) and Basic Research Fund for Central Public Research Institutes (No. 2017050, No.2017028).

References

[1] J.E. Cadotte, Interfacially synthesized reverse osmosis membrane, US, 1981.
[2] M. Prisciandaro, Reverse osmosis membranes for treatment of produced water: a process analysis, Desal. Water Treat., 55 (2015) 565–574.
[3] A. Rodríguezcalvo, G.A. Silvacastro, F. Osorio, J. González-zlópez, C. Calvo, Reverse osmosis seawater desalination: current status of membrane systems, Desal. Water Treat., 56 (2015) 849–861.
[4] M.T. Khan, M. Busch, V.G. Molina, A.H. Emwas, C. Aubry, J.P. Croue, How different is the composition of the fouling layer of wastewater reuse and seawater desalination RO membranes?, Water Res., 59 (2014) 271–282.
[5] V.G. Molina, M. Taub, L. Yohay, M. Busch, Long term membrane process and performance in Ashkelon Seawater Reverse Osmosis Desalination Plant, Desal. Water Treat., 31 (2011) 115–120.
[6] S.P. Chesters, Innovations in the inhibition and cleaning of reverse osmosis membrane scaling and fouling, Desalination, 238 (2009) 22–29.
[7] C.Y. Tang, T.H. Chong, A.G. Fane, Colloidal interactions and fouling of NF and RO membranes: A review, Adv. Colloid Interface Sci., 164 (2011) 126–143.
[8] L. Malaeb, G.M. Ayoub, Reverse osmosis technology for water treatment: State of the art review, Desalination, 267 (2011) 1–8.
[9] H.C. Flemming, Reverse osmosis membrane biofouling, Exp. Therm. Fluid Sci., 14 (1997) 382–391.
[10] E. Bendov, E. Bendavid, R. Messalem, M. Herzberg, A. Kushmaro, Biofilm formation on RO membranes: the impact of seawater pretreatment, Desal. Water Treat., 57 (2016) 4741–4748.
[11] A. Matin, Z. Khan, S.M.J. Zaidi, M.C. Boyce, Biofouling in reverse osmosis membranes for seawater desalination: Phenomena and prevention, Desalination, 281 (2011) 1–16.
[12] A. Belila, J. El-Chakhtoura, N. Otaibi, G. Muyzer, G. Gonzalez-Gil, P.E. Saikaly, M.C. van Loosdrecht, J.S. Vrouwenvelder, Bacterial community structure and variation in a full-scale seawater desalination plant for drinking water production, Water Res., 94 (2016) 62–72.

[13] S.H. Jia, L.N. Sim, J. Gu, R.D. Webster, A.G. Fane, H.G.L. Coster, A threshold flux phenomenon for colloidal fouling in reverse osmosis characterized by transmembrane pressure and electrical impedance spectroscopy, J. Membr. Sci., 500 (2016) 55–65.
[14] S. Jiang, Y. Li, B.P. Ladewig, A review of reverse osmosis membrane fouling and control strategies, Sci. Total Environ., 595 (2017) 567–583.
[15] G. Zhao, W.N. Chen, Design of poly(vinylidene fluoride)-g-p(hydroxyethyl methacrylate-co-N -isopropylacrylamide) membrane via surface modification for enhanced fouling resistance and release property, Appl. Surf. Sci., 398 (2017) 103–115.
[16] Y.F. Mi, Q. Zhao, Y.L. Ji, Q.F. An, C.J. Gao, A novel route for surface zwitterionic functionalization of polyamide nanofiltration membranes with improved performance, J. Membr. Sci., 490 (2015) 311–320.
[17] V. Kochkodan, D.J. Johnson, D.J. Johnson, N. Hilal, Polymeric membranes: surface modification for minimizing (bio)colloidal fouling, Adv. Colloid Interface Sci., 206 (2014) 116–140.
[18] S. Azari, L. Zou, E. Cornelissen, Assessing the effect of surface modification of polyamide RO membrane by l-DOPA on the short range physiochemical interactions with biopolymer fouling on the membrane, Colloids Surf. B, 120 (2014) 222–228.
[19] Y. Wang, Z. Wang, X. Han, J. Wang, S. Wang, Improved flux and anti-biofouling performances of reverse osmosis membrane via surface layer-by-layer assembly, J. Membr. Sci., 539 (2017) 403–411.
[20] G.D. Kang, Y.M. Cao, Development of antifouling reverse osmosis membranes for water treatment: A review, Water Res., 46 (2012) 584–600.
[21] G. Kang, M. Liu, B. Lin, Y. Cao, Q. Yuan, A novel method of surface modification on thin-film composite reverse osmosis membrane by grafting poly(ethylene glycol), Polymer, 48 (2007) 1165–1170.
[22] M. Safarpour, A. Khataee, V. Vatanpour, Thin film nanocomposite reverse osmosis membrane modified by reduced graphene oxide/TiO_2 with improved desalination performance, J. Membr. Sci., 489 (2015) 43–54.
[23] H. Zhao, Q. Shi, L. Wu, L. Zhang, H. Chen, C. Gao, Improving the performance of polyamide reverse osmosis membrane by incorporation of modified multi-walled carbon nanotubes, J. Membr. Sci., 450 (2014) 249–256.
[24] C.Y. Tang, Y.N. Kwon, J.O. Leckie, Effect of membrane chemistry and coating layer on physiochemical properties of thin film composite polyamide RO and NF membranes: II. Membrane physiochemical properties and their dependence on polyamide and coating layers, Desalination, 242 (2009) 168–182.
[25] W.L. Chou, D.G. Yu, M.C. Yang, The preparation and characterization of silver-loading cellulose acetate hollow fiber membrane for water treatment, Polym. Adv. Technol., 16 (2010) 600–607.
[26] B. Naik, V. Desai, M. Kowshik, G.F. Fernando, N.N. Ghosh, Synthesis of Ag/AgCl–mesoporous silica nanocomposites using a simple aqueous solution-based chemical method and a study of their antibacterial activity on E. coli, Particuology, 9 (2011) 243–247.
[27] T.S. Dhas, V.G. Kumar, V. Karthick, K.J. Angel, K. Govindaraju, Facile synthesis of silver chloride nanoparticles using marine alga and its antibacterial efficacy, Spectrochim. Acta Part A, 120 (2014) 416–420.
[28] J. Yin, Y. Yang, Z. Hu, B. Deng, Attachment of silver nanoparticles (AgNPs) onto thin-film composite (TFC) membranes through covalent bonding to reduce membrane biofouling, J. Membr. Sci., 441 (2013) 73–82.
[29] H.L. Yang, C.T. Lin, C. Huang, Application of nanosilver surface modification to RO membrane and spacer for mitigating biofouling in seawater desalination, Water Res., 43 (2009) 3777–3786.
[30] C. Zhou, D. Ye, H. Jia, S. Yu, M. Liu, C. Gao, Surface mineralization of commercial thin-film composite polyamide membrane by depositing barium sulfate for improved reverse osmosis performance and antifouling property, Desalination, 351 (2014) 228–235.
[31] S.H. Zhi, L.S. Wan, Z.K. Xu, Poly(vinylidene fluoride)/poly(acrylic acid)/calcium carbonate composite membranes via mineralization, J. Membr. Sci., 454 (2014) 144–154.
[32] H. Li, L. Peng, Y. Luo, P. Yu, Enhancement in membrane performances of a commercial polyamide reverse osmosis membrane via surface coating of polydopamine followed by the grafting of polyethylenimine, RSC Adv., 5 (2015) 98566–98575.
[33] S. Azari, L. Zou, Fouling resistant zwitterionic surface modification of reverse osmosis membranes using amino acid l -cysteine, Desalination, 324 (2013) 79–86.
[34] Y. Matsumura, K. Yoshikata, S. Kunisaki, T. Tsuchido, Mode of bactericidal action of silver zeolite and its comparison with that of silver nitrate, Appl. Environ. Microbiol., 69 (2003) 4278–4281.
[35] O. Choi, K.K. Deng, N.J. Kim, R.L. Jr, R.Y. Surampalli, Z. Hu, The inhibitory effects of silver nanoparticles, silver ions, and silver chloride colloids on microbial growth, Water Res., 42 (2008) 3066–3074.
[36] M. Zhang, B. Zhang, X. Li, Z. Yin, X. Guo, Synthesis and surface properties of submicron barium sulfate particles, Appl. Surf. Sci., 258 (2011) 24–29.
[37] X. Zhu, R. Bai, K.H. Wee, C. Liu, S.L. Tang, Membrane surfaces immobilized with ionic or reduced silver and their anti-biofouling performances, J. Membr. Sci., 363 (2010) 278–286.
[38] I.H. Huisman, P. Prádanos, A. Hernández, The effect of protein–protein and protein–membrane interactions on membrane fouling in ultrafiltration, J. Membr. Sci., 179 (2000) 79–90.
[39] D.J. Hughes, Z. Cui, R.W. Field, U.K. Tirlapur, In situ three-dimensional characterization of membrane fouling by protein suspensions using multiphoton microscopy, Langmuir, 22 (2006) 6266–6272.